A graphene oxide layer as an acid-resisting barrier deposited on a zeolite LTA membrane for dehydration of acetic acid†

Kai Xu, Zhenqi Jiang, Bo Feng and Aisheng Huang*

It is well known that zeolite LTA membranes have poor acid resistance although they have been considered the best hydrophilic zeolite membranes for the dehydration of organic aqueous mixtures. In the present work, we develop a simple and effective road to enhance the acidic stability of the zeolite LTA membrane through the depositing of a graphene oxide (GO) layer as an acid-resisting barrier on the surface of the zeolite LTA membrane. A relatively thin (about 5.5 μm) but dense and firm LTA@GO composite membrane is obtained by using dopamine as a covalent linker between the zeolite LTA and GO layers. The presence of the protective GO layer effectively inhibits the degradation of the zeolite LTA membrane by acetic acid, which greatly enhances its acid-resistant stability, leading to a high selectivity and stability for the dehydration of acetic acid. For the separation of 95 wt% acetic acid/water mixture at 333 K, the separation factor and flux of the LTA@GO composite membrane are about 400 and 1.5 kg m^{-2} h^{-1}, respectively, and keep almost constant for 168 h.

Introduction

In the past two decades, as a new type of inorganic membrane material, zeolite membranes have drawn more and more attention.[1–3] Attributing to their uniform pore size, excellent catalytic performance and high thermal stability, zeolite membranes are widely used as separators, reactors, sensors, electrical insulators, and microelectronics.[4–10] So far, zeolite LTA,[11–13] FAU (X and Y),[14,15] T-type,[16–18] MOR,[19,20] MFI (ZSM-5 and silicalite-1)[21–23] membranes have been synthesized on different supports. Among these zeolite membranes, only zeolite LTA membranes have been developed in an industrial-scale for the de-watering of bio-ethanol.[24] For the most of the aluminosilicate zeolite membranes, it is well recognized that the hydrophilicity of the zeolite membranes is enhanced with the increase of aluminum content, while the resistance to acid is weakened.[25,26] For example, the zeolite LTA membrane with Si/Al of 1.0 displays a strong hydrophilicity, but quickly lose its separation ability in 10 min when 1.0 mL sulfuric acid is added into a feed mixture of water/ethanol (50/50).[27]

However, there are many separation processes and chemical reactions which are completed in acid medium.[28–30] Therefore, the development of acid-stable and durable zeolite membranes is high desired for chemical engineering. Recently, various zeolite membranes with medium Si/Al ratio, such as T-type, MOR and ZSM-5, have been developed to meet the growing demand for the separation of acid/water solution. In comparison with the zeolite LTA membranes, these zeolite membranes show a higher stability in acid medium, but with moderate selectivity due to less hydrophilicity.[19,20,31–38] Surprisingly, most works to date focus on the development of new acid-stable membranes, but no reports on how to protect the zeolite LTA membrane away from the degradation in acid medium.

Recently, two-dimensional graphene has attracted intense interest due to its unique properties and potential applications.[39–42] Bao and colleagues reported that the encapsulating of CoNi nanoalloy by using ultrathin graphene shells is helpful to prevent the metal nanoparticles from directly exposing to the acidic media, and thus avoiding the deactivation of the catalyst.[43] Inspired by this novel concept, in the present work, a dense graphene oxide (GO) layer is deposited on the zeolite LTA membrane as an acid-resisting barrier. On one hand, as a graphene derivative prepared by deep chemical oxidation of graphite using strong acid and oxidants,[44] the GO layer shows high stable in the acid medium. On the other hand, there are abundant oxygen-containing groups in the GO framework, such as hydroxyl, epoxide, carboxyl and carbonyl groups, thus the GO layer shows preferential water adsorption ability and fast water diffusivity.[45–47] Further, with control of the spacing between GO nanosheets, ions or molecules can be effectively separated by ionic or molecular sieving.[47,48] Therefore, through the shielding of GO layer against the corrosion of acetic acid, it can be expected that the acid-resistant stability of the zeolite LTA

Institute of New Energy Technology, Ningbo Institute of Materials Technology and Engineering, Chinese Academy of Sciences, 1219 Zhongguan Road, 315201 Ningbo, P. R. China. E-mail: huangaisheng@nimte.ac.cn

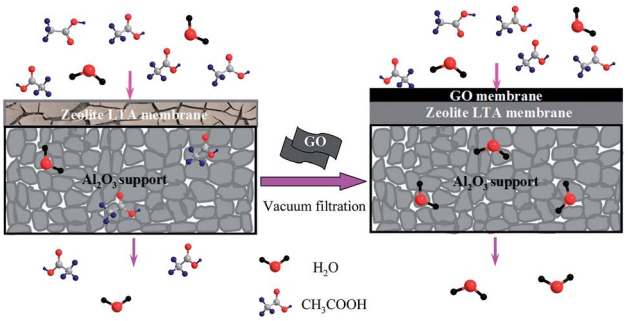

Fig. 1 Schematic diagram of the depositing of a graphene oxide (GO) layer as acid-resisting barrier on the surface of zeolite LTA membrane for the dehydration of acetic acid.

membrane can be great enhanced, thus resulting in a high selectivity and stability for the dehydration of acetic acid (Fig. 1).

Experimental

Materials

Chemicals were used as received: GO slurry (2.5 wt%, offered by Prof. Z. Liu of NIMTE); LUDOX AS-40 colloidal silica (40% SiO_2 in water, Aldrich); aluminum foil (99.99%, Aldrich); sodium hydroxide (>98%, Aladdin); dopamine (DPA, 98%, Aldrich); tris(hydroxymethyl) aminomethane (Tris–HCl, 99%, Aladdin); doubly distilled water. Porous α-Al_2O_3 disks (Fraunhofer Institute IKTS, former HITK/Inocermic, Hermsdorf, Germany: 18 mm in diameter, 1.0 mm in thickness, 70 nm particles in the top layer) were used as supports.

Preparation of zeolite LTA membranes on the PDA-modified α-Al_2O_3 disks

Before the hydrothermal synthesis of the bottom zeolite LTA membranes, the porous α-Al_2O_3 disks were treated with dopamine at 20 °C for 20 h.[11,49–51] Typically, DPA (2 mg mL^{-1}) was dissolved in 10 mM Tris–HCl (pH: 8.5) in an open watch glass (diameter: 180 mm). Then the top surface of the porous α-Al_2O_3 disks was treated with dopamine at 20 °C for 20 h, leading to PDA layer deposited on the support surface. For the synthesis of zeolite LTA membranes, a clear synthesis solution with the molar ratio of $50Na_2O : 1Al_2O_3 : 5SiO_2 : 1000H_2O$, was prepared according to the procedure reported elsewhere.[11–13] The aluminate solution was prepared by dissolving 22.22 g sodium hydroxide in 50 g deionized water, then adding 0.3 g aluminum foil to the solution at room temperature. The silicate solution was prepared by mixing 4.17 g LUDOX AS-40 colloidal silica and 47.5 g deionized water at 333 K with vigorous stirring. The prepared aluminum solution was added into the silicate solution with stirring for 20 h to produce a clear, homogenous solution. The PDA-modified α-Al_2O_3 disks were horizontally placed face down in a Teflon-lined stainless steel autoclave, and then the synthesis solution was poured into the autoclave. After *in situ* growth for 24 h at 333 K, the solution was decanted off and the zeolite LTA membrane was washed with deionized water several times, and then dried in air at 383 K over night for next step, characterization and pervaporation.

Preparation of sandwich-structured LTA@GO composite membrane

The as-synthesized zeolite LTA membrane was treated with dopamine according to the above procedure. For the fabrication of GO protective layer on the PDA-modified zeolite LTA membrane, 1 g GO slurry was dissolved in 50 mL deionized water to obtain 0.5 mg mL^{-1} GO suspension. The resulting GO suspension was treated ultrasonically several hours to form GO nanosheets. Afterwards, 3 mL as-prepared GO suspension was added on the top surface of the PDA-modified zeolite LTA membrane which was mounted in a home-made model. After water evaporation with vacuum-assisted filtration at 333 K, the GO layer was deposited on the surface of the zeolite LTA membrane to prepare LTA@GO composite membrane. And then, the LTA@GO composite membrane was dried in an oven at 333 K over night.

Characterization of zeolite LTA and LTA@GO composite membranes

The morphology and thickness of the zeolite LTA and LTA@GO composite membranes were characterized by field emission scanning electron microscopy (FESEM). FESEM were taken on an S-4800 (Hitachi) with a cold field emission gun operated at 4 kV and 10 μA. The phase purity and crystallinity of the LTA and LTA@GO composite membrane were confirmed by X-ray diffraction (XRD). The XRD patterns were recorded at ambient conditions with Bruker D8 ADVANCE X-ray diffractometer with Cu Kα radiation at 40 kV and 40 mA. The functional groups of GO powders were measured by an FT-IR spectrum (Nicolet 6700, Thermo Scientific, USA).

Separation of acetic acid/water by pervaporation

The separation performances of the zeolite LTA membrane and LTA@GO composite membrane were evaluated by pervaporation for dehydration of 95 wt% acetic acid/water mixtures at 333 K, the apparatus used for the pervaporation experiments is illustrated schematically elsewhere.[50] For the pervaporation experiments, the membranes were sealed in a home-made permeation cell with silicone O-rings, and the whole membrane module was heated in a thermostatic water bath together with the feed solution. The permeate side of the membrane was evacuated by using a vacuum pump. Two freezing traps with liquid N_2 cooling were used to collect the permeate at every time interval. The compositions of the feed and the permeate were analyzed by gaschromatography (GC-1690T, Jiedao).

The most important variables for pervaporation are the selectivity and the flux. The total flux (J) and the separation factor (α) are defined as follows.

$$J = \frac{W}{\Delta t \cdot A}$$

$$\alpha_{i/j} = \frac{x_{ip}}{x_{if}} \cdot \frac{x_{jf}}{x_{jp}}$$

where W is total weight of the permeate (kg), Δt is collecting time (h), A is separation area of the membrane (m^2), x_{ip} is the weight fraction of species i in the permeate and x_{if} is the weight fraction of species i in the feed.

Results and discussion

Preparation and characterization of the zeolite LTA membrane

Fig. 2a and b show the FESEM images of the zeolite LTA membrane prepared on the PDA-modified α-Al_2O_3 disk. In good agreement with our previous report,[11] the surface of the PDA-modified α-Al_2O_3 disk is completely covered by uniform and compact cubic-shaped LTA crystals, forming a dense zeolite LTA membrane, and no visible cracks, pinholes or other macroscopic defects are observed (Fig. 2a). From the cross-section view (Fig. 2b), it can be seen that the zeolite LTA membrane is well intergrown with a thin thickness of about 4.0 μm. The formation of a phase-pure zeolite LTA membrane with a high degree of crystallinity was confirmed by XRD (Fig. 3c), which indicates that all peaks match well with those of zeolite LTA powder besides the α-Al_2O_3 signals from the support (Fig. 3a and b). As reported previously,[11,49] attributing to the excellently adhesive ability through the formation of covalent bonds, zeolite LTA nutrients are easily attracted and bound to the support surface, thus facilitating the nucleation and growth of uniform, well intergrown and phase-pure zeolite LTA membranes.

Preparation and characterization of the LTA@GO composite membrane

Fig. 2c and d show the FESEM images of the LTA@GO composite membrane prepared on the α-Al_2O_3 disk. After deposition of GO suspension by vacuum-assisted filtration on the PDA-modified zeolite LTA membrane, a dense GO layer with typical wavy wrinkles is formed on the PDA-modified zeolite LTA membrane, and no cracks, pinholes or other visible defects are found in the GO layer (Fig. 2c). From the cross-section view shown in Fig. 2d, the GO layer with a thickness of about 1.5 μm is closely stuck on the surface of the zeolite LTA membrane, thus forming a sandwich-structured LTA@GO composite membrane. The formation of LTA@GO composite membrane was confirmed by XRD analysis. As shown in Fig. 3e, both zeolites LTA and GO peaks are clearly observed in the XRD pattern, and all the detected peaks match well with those of LTA and GO besides the Al_2O_3 signals from the support.

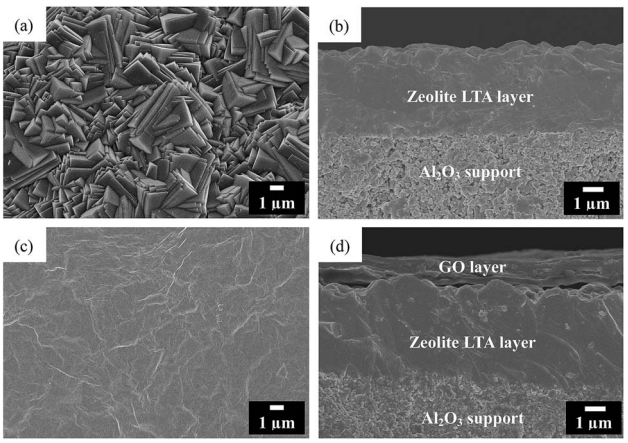

Fig. 2 Top view (a) and cross-section view (b) FESEM images of the zeolite LTA membrane prepared on a PDA-modified Al_2O_3 disk; top view (c) and cross-section view (d) FESEM images of the LTA@GO composite membrane.

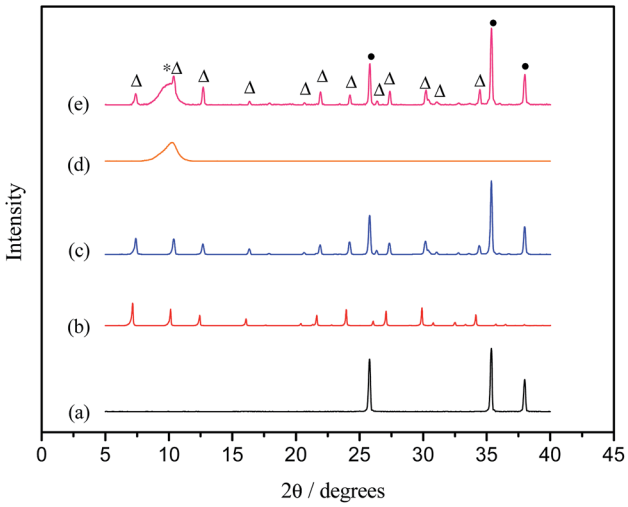

Fig. 3 XRD patterns of the PDA-modified α-Al_2O_3 support (a), zeolite LTA powder (b), zeolite LTA membrane on a PDA-modified α-Al_2O_3 support (c), GO powder (d), and LTA@GO composite membrane on α-Al_2O_3 support (e). (Δ): zeolite LTA, (*): GO, (●): α-Al_2O_3 support.

It is found that the PDA modification of the surface of the as-prepared zeolite LTA membrane is indispensable to prepare compact and stable LTA@GO composite membrane. As shown in (Fig. S1†), when the surface of the as-prepared zeolite LTA membrane was not modified with PDA before the deposition of GO layer, observable gaps can be seen due to weak interaction between the GO layer and as-prepared zeolite LTA layer. Therefore, the GO layer easily peel off from the surface of the as-prepared zeolite LTA membrane, which is harmful to the separation performance of the LTA@GO membrane. Through the PDA modification of the as-prepared zeolite LTA membrane, the GO nanosheets can be firmly stuck onto the surface of the zeolite LTA membrane due to the formation of strongly covalent bonds between PDA and GO (Fig. S2†), leading to the formation of dense and stable LTA@GO membrane.

Separation of acetic acid/water by pervaporation

It is well known that the zeolite LTA membranes are unstable in the acidic solution.[27,52] Fig. 4 shows the separation performances of the zeolite LTA membrane as a function of the pervaporation time for the separation of 95 wt% acetic acid/water mixture at 333 K. It can be seen that the separation factor of the

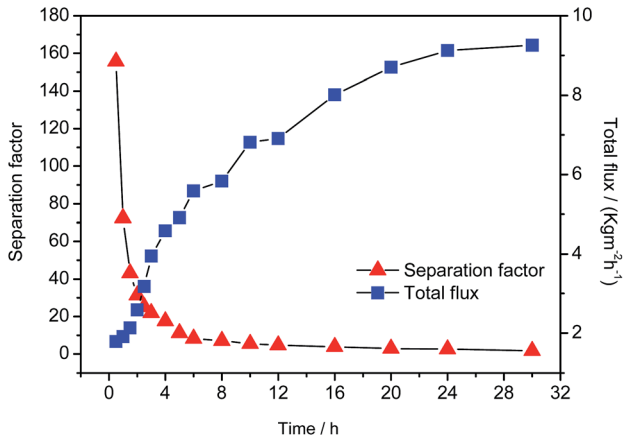

Fig. 4 Separation factor and total flux of the zeolite LTA membrane as a function of the operation time for the separation of 95 wt% acetic acid/water mixture by pervaporation at 333 K.

zeolite LTA membrane is as high as 156 in the first half an hour, but sharply decreases to only 11 after 5 h, and finally decreases to 1. Accordingly, the total flux remarkably increases from 1.8 to 9.2 kg m^{-2} h^{-1}. Fig. 5 shows the morphology changes of the zeolite LTA membrane as a function of the testing time in contact with 95 wt% acetic acid/water mixture at 333 K. It can be seen clearly that the zeolite LTA membrane begins to dissolve and form observable cracks when the zeolite LTA membrane is immerse in the acetic acid for only 1 h, and finally the cubic-shaped LTA crystals are completely changed into a snowflake-shaped amorphous after 24 h. These results suggest that the zeolite LTA membrane has been damaged and lost the separation performance in a very short time due to its instability in the acidic solution.

On the contrary, when a GO layer was deposited as an acid-resisting barrier on the surface of the zeolite LTA membrane, the separation performance of the zeolite LTA membrane can remain unchanged for a long time. Fig. 6 shows the separation performances of the LTA@GO composite membrane as a function of the pervaporation time for the separation of 95 wt% acetic acid/water mixture at 333 K. As shown in Fig. 6, the separation factor of the LTA@GO membrane is about 400, with total flux of about 1.55 kg m^{-2} h^{-1}. Comparing with literature data of the separation of acetic acid/water mixture, the LTA@GO composite membrane developed in this study is among those with high separation performances (Table S1†). Further, both the separation factor and the total flux keep almost unchanged for a long time of 168 h, suggesting that acid-resistant stability of the zeolite LTA membrane can be greatly enhanced through the shielding of GO layer against the corrosion of acetic acid. Attributing to the preferential water adsorption ability and fast water diffusivity, probably the water molecules (2.6 Å) can pass through the GO membrane, while the hydrated hydrogen ions (2.8 Å) are excluded to go through the GO membrane. Therefore, the degradation of the zeolite LTA membrane is avoided due to the insulation of acetic acid, resulting in a high stability for the dehydration of acetic acid.

In good agreement with the high stability for the dehydration of acetic acid, in comparison with the as-prepared LTA@GO membrane, there are no obvious differences in the FESEM images (Fig. 7) and XRD pattern (Fig. S3†) after the measurement of dewatering of acetic acid by pervaporation for 168 h at 333 K, further confirming that the LTA@GO composite membrane has a high acid-resistant stability. It should be noted that even for the high silicon zeolite membranes such as MOR and ZSM-5, their acid resistance can not always remain unchanged for long time.[33,36] In the present work, since GO is extremely stable under acidic solutions, the LTA@GO composite membrane displays a high acid-resistant ability with the protection of GO layer. Therefore, the concept of GO as

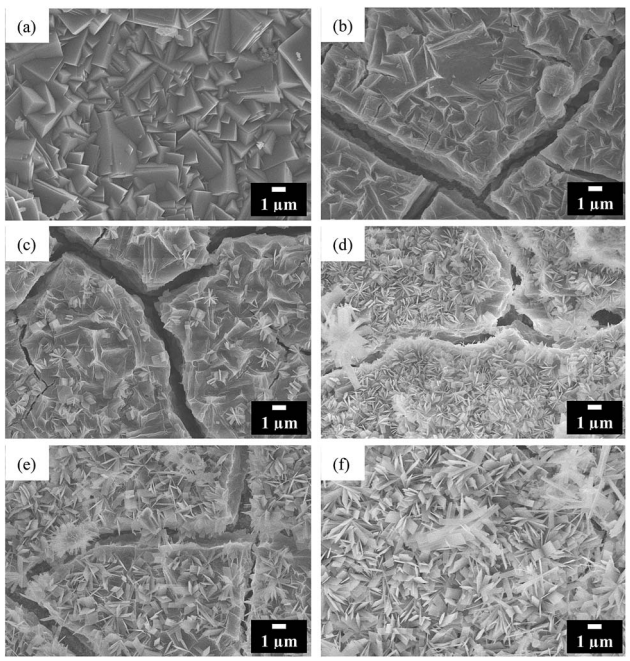

Fig. 5 FESEM images of the zeolite LTA membranes which were immersed in 95 wt% acetic acid/water mixtures at 333 K with different time: 0 h (a), 1 h (b), 4 h (c), 8 h (d), 16 h (e) and 24 h (f).

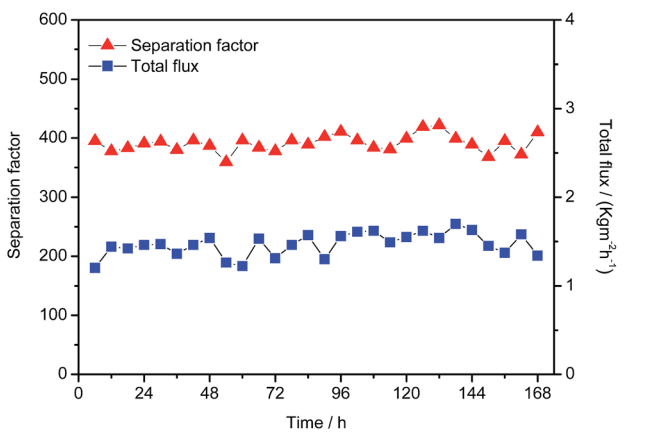

Fig. 6 Separation factor and total flux of the LTA@GO composite membrane as a function of the operation time for the separation of 95 wt% acetic acid/water mixture by pervaporation at 333 K.

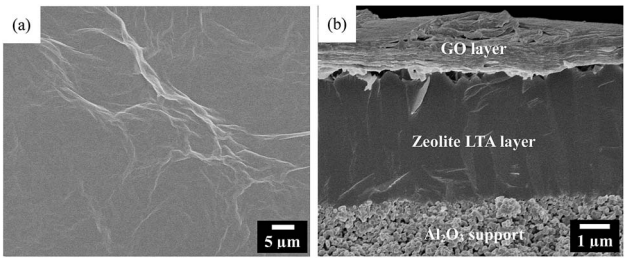

Fig. 7 Top view (a) and cross-section (b) FESEM images of the LTA@GO composite membrane after the separation of 95 wt% acetic acid/water mixture by pervaporation for 168 h at 333 K.

a protective layer will open a new door to solve the problem of the poor acid stability of the zeolite LTA membrane.

Conclusions

In conclusion, in the present work we have developed a sandwich-structured LTA@GO composite membrane by using polydopamine as molecular linker. The GO top layer acts as a protective layer to avoid the direct contact between zeolite LTA membrane and acidic solution. Through the shielding of GO layer against the corrosion of acetic acid, the acid-resistant stability of the zeolite LTA membrane can be enhanced greatly, leading to a high selectivity and stability for the dehydration of acetic acid. For the separation of 95 wt% acetic acid/water mixture at 333 K, both the separation factor (about 400) and total flux (about 1.55 kg m^{-2} h^{-1}) of the LTA@GO composite membrane remain unchanged for 168 h. The high separation performances combined with high stability and facile fabrication road recommend the developed LTA@GO membrane as a promising candidate for the dehydration of organic aqueous mixtures in acid medium.

Acknowledgements

Financial support by National Natural Science Foundation of China (21576273, 21276262), External Cooperation Program of BIC, CAS (174433KYSB2013005), National High Technology Research and Development Program of China (2015AA03A602), and Ningbo Science and Technology Innovation Team (2014B81004).

References

1 N. Rangnekar, N. Mittal, B. Elyassi, J. Caro and M. Tsapatsis, *Chem. Soc. Rev.*, 2015, **44**, 7128–7154.
2 Z. Y. Yeo, T. L. Chew, P. W. Zhu, A. R. Mohamed and S. P. Chai, *J. Porous Mater.*, 2013, **20**, 1457–1475.
3 M. Yu, R. D. Noble and J. L. Falconer, *Acc. Chem. Res.*, 2011, **44**, 1196–1206.
4 J. Caro and M. Noack, *Microporous Mesoporous Mater.*, 2008, **115**, 215–233.
5 Y. Lin, *Sep. Purif. Technol.*, 2001, **25**, 39–55.
6 A. Tavolaro and E. Drioli, *Adv. Mater.*, 1999, **11**, 975–996.
7 E. E. McLeary, J. C. Jansen and F. Kapteijn, *Microporous Mesoporous Mater.*, 2006, **90**, 198–220.
8 M. Yu, J. L. Falconer, T. J. Amundsen, M. Hong and R. D. Noble, *Adv. Mater.*, 2007, **19**, 3032–3036.
9 Z. Wang, H. Wang, A. Mitra, L. Huang and Y. Yan, *Adv. Mater.*, 2001, **13**, 746–749.
10 M. P. Pina, R. Mallada, M. Arruebo, M. Urbiztondo, N. Navascues, O. de la Iglesia and J. Santamaria, *Microporous Mesoporous Mater.*, 2011, **144**, 19–27.
11 C. Yuan, Q. Liu, H. Chen and A. Huang, *RSC Adv.*, 2014, **4**, 41982–41988.
12 B. Huang, Q. Liu, J. Caro and A. Huang, *J. Membr. Sci.*, 2014, **455**, 200–206.
13 A. Huang, F. Liang, F. Steinbach and J. Caro, *J. Membr. Sci.*, 2010, **350**, 5–9.
14 A. Huang, N. Wang and J. Caro, *J. Membr. Sci.*, 2012, **389**, 272–279.
15 J. C. White, P. K. Dutta, K. Shqau and H. Verweij, *Langmuir*, 2010, **26**, 10287–10293.
16 F. Zhang, Y. Zheng, L. Hua, N. Hu, M. Zhu, R. Zhou, X. Chen and H. Kita, *J. Membr. Sci.*, 2014, **456**, 107–116.
17 X. Wang, Z. Yang, C. Yu, L. Yin, C. Zhang and X. Gu, *Microporous Mesoporous Mater.*, 2014, **197**, 17–25.
18 R. Zhou, L. Hu, Y. Zhang, N. Hu, X. Chen, X. Lin and H. Kita, *Microporous Mesoporous Mater.*, 2013, **174**, 81–89.
19 M. Zhu, S. Xia, X. Hua, Z. Feng, N. Hu, F. Zhang, I. Kumakiri, Z. Lu, X. Chen and H. Kita, *Ind. Eng. Chem. Res.*, 2014, **53**, 19168–19174.
20 Y. Zhang, Y. Nakasaka, T. Tago, A. Hirata, Y. Sato and T. Masuda, *Microporous Mesoporous Mater.*, 2015, **207**, 39–45.
21 Y. Peng, X. Lu, Z. Wang and Y. Yan, *Angew. Chem., Int. Ed.*, 2015, **54**, 5709–5712.
22 Y. Peng, H. Lu, Z. Wang and Y. Yan, *J. Mater. Chem. A*, 2014, **2**, 16093–16100.
23 M. Tawalbeh, F. H. Tezel, B. Kruczek, S. Letaief and C. Detellier, *J. Porous Mater.*, 2013, **20**, 1407–1421.
24 Y. Morigami, M. Kondo, J. Abe, H. Kita and K. Okamoto, *Sep. Purif. Technol.*, 2001, **25**, 251–260.
25 M. Matsukata, K. i. Sawamura, T. Shirai, M. Takada, Y. Sekine and E. Kikuchi, *J. Membr. Sci.*, 2008, **316**, 18–27.
26 S. L. Wee, C. T. Tye and S. Bhatia, *Sep. Purif. Technol.*, 2008, **63**, 500–516.
27 Y. Hasegawa, T. Nagase, Y. Kiyozumi, T. Hanaoka and F. Mizukami, *J. Membr. Sci.*, 2010, **349**, 189–194.
28 Z. Chen, J. Yang, D. Yin, Y. Li, S. Wu, J. Lu and J. Wang, *J. Membr. Sci.*, 2010, **349**, 175–182.
29 X. Peng, Q. Lei, G. Lv and X. Zhang, *Sep. Purif. Technol.*, 2012, **89**, 84–90.
30 S. Guo, B. He, J. Li, Q. Zhao and Y. Cheng, *Chem. Eng. Technol.*, 2014, **37**, 478–482.
31 G. Li, E. Kikuchi and M. Matsukata, *Sep. Purif. Technol.*, 2003, **32**, 199–206.
32 S. G. Li, V. A. Tuan, R. D. Noble and J. L. Falconer, *Ind. Eng. Chem. Res.*, 2001, **40**, 6165–6171.
33 M. H. Zhu, I. Kumakiri, K. Tanaka and H. Kita, *Microporous Mesoporous Mater.*, 2013, **181**, 47–53.

34 K. Sato, K. Sugimoto, T. Kyotani, N. Shimotsuma and T. Kurata, *Microporous Mesoporous Mater.*, 2012, **160**, 85–96.
35 K. Sato, K. Sugimoto, T. Kyotani, N. Shimotsuma and T. Kurata, *J. Membr. Sci.*, 2011, **385**, 20–29.
36 X. Li, H. Kita, H. Zhu, Z. Zhang and K. Tanaka, *J. Membr. Sci.*, 2009, **339**, 224–232.
37 J. Yang, L. Li, W. Li, J. Wang, Z. Chen, D. Yin, J. Lu, Y. Zhang and H. Guo, *Chem. Commun.*, 2014, **50**, 14654–14657.
38 K. Tanaka, R. Yoshikawa, C. Ying, H. Kita and K. Okamoto, *Catal. Today*, 2001, **67**, 121–125.
39 K. S. Novoselov, A. K. Geim, S. V. Morozov, D. Jiang, Y. Zhang, S. V. Dubonos, I. V. Grigorieva and A. A. Firsov, *Science*, 2004, **306**, 666–669.
40 S. Stankovich, D. A. Dikin, G. H. B. Dommett, K. M. Kohlhaas, E. J. Zimney, E. A. Stach, R. D. Piner, S. T. Nguyen and R. S. Ruoff, *Nature*, 2006, **442**, 282–286.
41 A. K. Geim and K. S. Novoselov, *Nat. Mater.*, 2007, **6**, 183–191.
42 A. K. Geim, *Science*, 2009, **324**, 1530–1534.
43 J. Deng, P. Ren, D. Deng and X. Bao, *Angew. Chem., Int. Ed.*, 2015, **54**, 2100–2104.
44 G. Shao, Y. Lu, F. Wu, C. Yang, F. Zeng and Q. Wu, *J. Mater. Sci.*, 2012, **47**, 4400–4409.
45 D. R. Dreyer, S. Park, C. W. Bielawski and R. S. Ruoff, *Chem. Soc. Rev.*, 2010, **39**, 228–240.
46 K. Huang, G. Liu, Y. Lou, Z. Dong, J. Shen and W. Jin, *Angew. Chem., Int. Ed.*, 2014, **53**, 6929–6932.
47 R. K. Joshi, P. Carbone, F. C. Wang, V. G. Kravets, Y. Su, I. V. Grigorieva, H. A. Wu, A. K. Geim and R. R. Nair, *Science*, 2014, **343**, 752–754.
48 W. Hung, C. Tsou, M. De Guzman, Q. An, Y. Liu, Y. Zhang, C. Hu, K. Lee and J. Lai, *Chem. Mater.*, 2014, **26**, 2983–2990.
49 Q. Liu, N. Wang, J. Caro and A. Huang, *J. Am. Chem. Soc.*, 2013, **135**, 17679–17682.
50 Q. Liu, B. Huang and A. Huang, *J. Mater. Chem. A*, 2013, **1**, 11970–11974.
51 A. Huang, Q. Liu, N. Wang and J. Caro, *J. Mater. Chem. A*, 2014, **2**, 8246–8251.
52 T. Kyotani, N. Shimotsuma and S. Kakui, *Anal. Sci.*, 2006, **22**, 325–327.